RAPID COMMUNICATIONS

PHYSICAL REVIEW B VOLUME 43, NUMBER 16 1 JUNE 1991

# Critical surface of the Blume-Emery-Griffiths model on the honeycomb lattice

Leh-Hun Gwa
*Department of Mathematics, Rutgers University, New Brunswick, New Jersey 08903*

F. Y. Wu
*Department of Physics, Northeastern University, Boston, Massachusetts 02115*

(Received 14 March 1991)

We consider the Blume-Emery-Griffiths (BEG) model on the honeycomb lattice and obtain a closed-form expression for the critical surface of second-order transitions. The BEG model is first formulated as a three-state vertex model. Using the fact that the BEG critical surface coincides with that of a general three-state vertex model, we construct critical surfaces by forming polynomial combinations of vertex weights that are invariant under an O(3) gauge transformation. We then carry out a finite-size analysis of the BEG model, and use data so obtained to determine coefficients appearing in the polynomial combination. This procedure leads to a closed-form expression of the critical surface which reproduces all numerical data accurately.

The Blume-Emery-Griffiths (BEG) model[1] is a spin-1 system described by the (reduced) Hamiltonian

$$-\mathcal{H}/kT = J\sum_{\langle ij\rangle} S_iS_j + K\sum_{\langle ij\rangle} S_i^2S_j^2 - \Delta\sum_i S_i^2 , \qquad (1)$$

where $S_i = 0, \pm 1$. The model was first proposed to explain certain magnetic transitions.[2-4] It has also proven to be useful for modeling of the $\lambda$ transition in $^3$He-$^4$He mixtures[1] and the phase changes in a microemulsion.[5] An important feature of the critical behavior of the BEG model is the occurrence of a multicritical phenomenon accompanied with the onset of first- and second-order transitions.[6] However, studies of its phase diagram carried out in the past have been mostly by approximations, including renormalization-group[7] and mean-field[1,8,9] analyses, and Monte Carlo simulations.[10] An exact determination of its phase diagram has proven to be elusive, and has been limited to the subspaces $J=0$,[11,12] and $K=-\ln\cosh J$.[13-16] In this paper, we present results on a precise determination of the second-order phase surface for the BEG model (1) on the honeycomb lattice.

Our approach parallels that of recent progress made in the determination of the phase diagram for antiferromagnetic Ising models.[17-21] By using an invariance property in conjunction with results of a finite-size analysis, it has been possible to obtain closed-form expressions for the phase boundaries of the Ising models, which agree with all numerical data to an extremely high degree of precision.[17-19] For spin-1 systems such as the BEG model, the underlying invariance is that of an O(3) gauge transformation, whose properties have recently been studied.[22] Here we make use of these invariance properties and results of a finite-size analysis, which we carry out, to obtain closed-form expressions of the second-order transition phase boundary for the honeycomb BEG model.

We first formulate the BEG model as a three-state vertex model. Starting from the partition function of the BEG model,

$$Z_{\rm BEG} = \sum_{S_i=0,\pm1}\prod_{\langle ij\rangle}\exp(JS_iS_j + KS_i^2S_j^2)\prod_i e^{-\Delta S_i^2} , \qquad (2)$$

we write

$$\exp(JS_iS_j + KS_i^2S_j^2) = 1 + zS_iS_j + tS_i^2S_j^2 , \qquad (3)$$

where

$$z \equiv e^K\sinh J, \quad t \equiv e^K\cosh J - 1 , \qquad (4)$$

and expand the product $\prod_{\langle ij\rangle}$ in Eq. (2). For each term in the expansion for which the factor 1, $zS_iS_j$, or $tS_i^2S_j^2$ is taken, we draw, respectively, a dotted, heavy, or thin line over the corresponding lattice edge. Then $Z_{\rm BEG}$ generates graphs on the underlying lattice. Next we associate weights to lattice sites (vertices), obtained by carrying out the summations $\sum_{S_i=0,\pm1}$. Using the identities

$$\sum_{S_i=0,\pm1} S_i^n e^{-\Delta S_i^2} = \begin{cases} 2e^{-\Delta}+1, & n=0 \\ 2e^{-\Delta}, & n=\text{even} \\ 0, & n=\text{odd} , \end{cases} \qquad (5)$$

we see that only those vertices having an even number of incident heavy lines have nonzero weights. For the honeycomb lattice, this leads to a 14-vertex model shown in Fig. 1 with the weights

$$a=\omega_{300}=1+\tfrac{1}{2}e^{\Delta}, \quad b=\omega_{201}=t^{1/2}, \quad c=\omega_{102}=t ,$$
$$d=\omega_{003}=t^{3/2}, \quad f=\omega_{120}=z, \quad g=\omega_{021}=zt^{1/2} . \qquad (6)$$

Here, for convenience, we have multiplied a factor $e^{\Delta}/2$ to all vertex weights, and introduced the abbreviated notation $\omega_{ijk}$ to represent the weight of a vertex configuration with respective $i,j,k$ dotted, heavy, and thin lines.

The most general three-state vertex model for the honeycomb lattice is a 27-vertex model[22] which, in addition to the 14 vertices shown in Fig. 1, includes vertices with weights $\omega_{030}$, $\omega_{111}$, $\omega_{210}$, and $\omega_{012}$. The partition function of this general model is invariant under an O(3) gauge transformation. Furthermore, it has been shown that for threefold-coordinated lattices the O(3) gauge transformation possesses six fundamental invariants, and

 

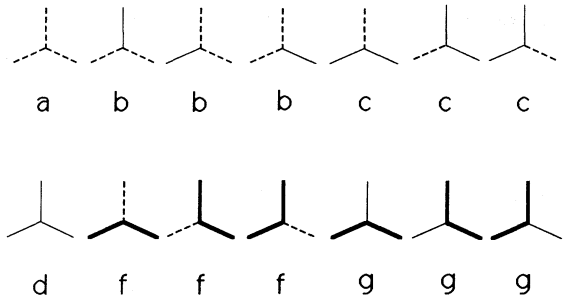


FIG. 1. Vertex configurations of the three-state 14-vertex model for the BEG model.

their explicit expressions have been given.[22] In the BEG subspace $\omega_{030}=\omega_{111}=\omega_{210}=\omega_{012}=0$, one of these fundamental invariants vanishes identically and the remaining five reduce to

$$\begin{aligned} I_0&=(a+c+f)^2+(b+d+g)^2\,,\\ J_1&=A+15B\,,\\ J_2&=C-B^2-AB\,,\\ J_3&=AC+3BC-2B^3-6AB^2\,,\\ J_4&=4(5A-9B)C^2+(A^3+21A^2B-93AB^2+135B^3)\\ &\quad+2B^2(9A^3-59A^2B+99AB^2-81B^3)\,, \end{aligned} \tag{7}$$

where

$$\begin{aligned} &A=-e_0e_0^*,\ B=-e_2e_2^*,\ C=-e_0^*e_2^3-e_0(e_2^*)^3\,,\\ &e_0=-a+3c+i(3b-d)\,,\\ &e_2=\tfrac{1}{5}[(a+c-4f)-i(b+d-4g)]\,. \end{aligned} \tag{8}$$

It should be emphasized that Eqs. (7) are intersections of fundamental invariants of the 27-vertex model in the BEG subspace, which are not themselves invariants for the BEG model. We shall, however, simply call $A$, $B$, and $C$ the invariants for convenience in ensuing discussions.

Generally, we expect critical surfaces of the 27-vertex model to be invariant under the O(3) gauge transformation. It follows that they must lie on subspaces whose explicit expressions are formed from the six fundamental invariants. For the BEG model, in particular, the phase boundaries are then given by expressions formed by the invariants $I_0$, $A$, $B$, and $C$. If we further assume that phase boundaries are given in terms of these expressions as homogeneous polynomials of the vertex weights, we are led to the following possible expressions for the phase boundaries:

$$\begin{aligned} &P_2\equiv I_0+c_1A+c_2B=0\,,\\ &P_4\equiv C+c_1I_0^2+c_2A^2+c_3B^2+c_4I_0A+c_5I_0B+c_6AB=0\,, \end{aligned} \tag{9}$$

and similar higher-degree polynomials, where the $c_j$'s are constants yet to be determined. Here, $P_n$ in Eq. (9) is a polynomial homogeneous in the $n$th degree of the vertex weights, and we apply the method of finite-size analysis to compute the coefficients $c_j$'s. First, for fixed ratios of $\Delta/K$ and $J/K$, we use finite-size scaling to determine the critical temperature $K_c=1/kT_c$. Values of $K_c$ so determined are then used in conjunction with (9) to determine the coefficients $c_j$'s from a least-squares fit.

The finite-size theory[23–25] of second-order transitions predicts that the correlation length at a critical point scales linearly with the linear dimension of the system $n$. The correlation length can be found by computing the first- and second-largest eigenvalues of the transfer matrix, $\lambda_1$ and $\lambda_2$, for a row of $n$ lattice sites. More precisely, we have

$$n\zeta\ln(\lambda_1/\lambda_2)=2\pi x_H\,, \tag{10}$$

with $\zeta$ a geometric factor and $x_H$ the magnetic scaling dimension. We compute $\lambda_1$ and $\lambda_2$ for the transfer matrix of the BEG model on a honeycomb lattice, taken in a direction perpendicular to one of the lattice edges.[26] The transfer matrix in this direction is symmetric and the geometric factor takes the value $\zeta=1/\sqrt{3}$.

A conjugate-gradient algorithm is used to search for the leading eigenvalues and eigenvectors. The leading eigenvector is contained in the subspace with all elements positive, as guaranteed by Perron-Frobenius theorem; the next largest eigenvalue is computed by confining the algorithm to the subspace orthogonal to the leading eigenvector. The latter procedure is carried out by choosing a random vector, and subtracting from it the component along the leading eigenvector, to ensure that the search covers the maximal subspace. This is in contrast to the usual procedure for the Ising model, where a symmetry known to hold in the next leading eigenvector is used explicitly in its construction.

A total of 205 data points for $n=2$, 4, 6 are collected from the finite-size calculation, using $x_H=\frac{1}{8}$ for the Ising universality class. A least-squares fit is then performed on the $n=6$ data to obtain the best values for the constants in the polynomial equations $P_2=0$ and $P_4=0$. The results are $c_1=-0.5996$ and $c_2=47.08$ for the second-degree equation, and $c_1=0.005\,260$, $c_2=0.095\,34$, $c_3=5.601$, $c_4=-0.070\,96$, $c_5=0.3708$, and $c_6=-3.374$ for the fourth-degree equation. The finite-size data and curves obtained from the polynomial equations (9) with coefficients determined in the above are plotted in Fig. 2. Considering the facts that this is a surface fitting and that there are no more than six adjustable constants, the fit is remarkably good. As a comparison, we have carried out a similar least-squares fit using fourth- and sixth-degree homogeneous polynomials constructed from the invariants (7). In this case, we find the best fits marked by ruptures across smooth data points, indicating that the fits are unsatisfactory. This finding also indicates that we are on the right track in choosing $I_0$, $A$, $B$, and $C$ as the building blocks of BEG invariants. We therefore suggest that the equation $P_4=0$ can be used as a good closed-form approximation for the second-order critical surface of the BEG model.

As an independent check of the accuracy of our results,

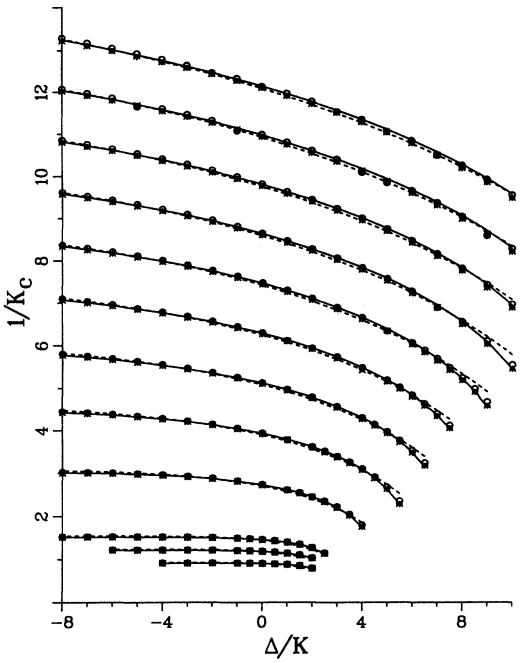


FIG. 2. Second-order phase boundary from finite-size analysis (○: $n=2$; ×: $n=4$; +: $n=6$), and from the polynomial equations $P_2=0$ (dashed line) and $P_4=0$ (solid line). The 12 branches are for $J/K=0.6, 0.8, 1, 2, 3, \ldots, 10$, in the order of increasing $1/K_c$.

we have used (9) to compute the critical point at $\Delta/K=2$, $J/K=\frac{1}{3}$, for which the BEG model (1) is known[27] to be equivalent to the three-state Potts model with nearest-neighbor interactions $2K/3$ and the exact critical point $K_c^{-1}=0.449\,175$. Using $P_4=0$ we obtain $K_c^{-1}=0.458\,756$. Considering that this point lies well beyond the regime of our data points and close to the first-order boundary, the agreement is very good.

Guided by the behavior of the phase diagram obtained under the mean-field approximation,[1] we expect, as $\Delta/K$ increases, the second-order lines in Fig. 2 to terminate and change into first-order lines at multicritical points. Indeed, results of our numerical fitting show that calculated values of the coefficients are very sensitive to input boundary data at the lower-right-hand corner of Fig. 2, signifying a changeover into a first-order surface (for which the finite-size scaling needs to be reformulated). Thus, the second-order surface given by (9) should terminate at a first-order surface rising in the lower-right-hand regime of Fig. 2.

Finally, we remark on how one might locate this first-order surface. Generally, again by invariance arguments, we expect the first-order surface to be also given in the form of (9). Furthermore, the intersection of the surface with the $J=0$ plane is exactly known.[11,12] In the plane $J=0$, the BEG model (1) is completely equivalent to an Ising model with interactions $K_I=K/4$ and a magnetic field $(\frac{3}{2}K-\Delta+\ln 2)/2$. The first-order boundary is then precisely the line segment $J=0$, $e^{\Delta}=2e^{3K/2}$, $e^{2K_I}=e^{K/2}\leq 2+\sqrt{3}$. In addition, from a ground-state energy analysis, one finds that the first-order surface contains the zero-temperature phase boundary $J/K+1=2\Delta/3K$. These exact intersections together with any precision determination of a few first-order transition points will then enable one to complete the picture of the full phase diagram.

This work is supported in part by NSF Grants No. DMR-8918903 and No. DMR-9015489. We would like to thank L. Y. Zhu for his interest during the initial stage of this work. We would also like to thank X. N. Wu for helpful discussions on the numerical procedure.

[1] M. Blume, V. J. Emery, and R. B. Griffiths, Phys. Rev. B **4**, 1071 (1971).
[2] M. Blume, Phys. Rev. **141**, 517 (1966).
[3] H. W. Capel, Physica **32**, 966 (1966); **33**, 795 (1967); **37**, 423 (1967).
[4] M. Blume and R. E. Watson, J. Appl. Phys. **38**, 991 (1967).
[5] M. Schick and W. Shih, Phys. Rev. B **34**, 1797 (1986).
[6] For a review of the tricritical behavior including that in the BEG model, see L. D. Lawrie and S. Sarbach, in *Phase Transitions and Critical Phenomena,* edited by C. Domb and J. L. Lebowitz (Academic, New York, 1984), Vol. 9.
[7] A. N. Berker and M. Wortis, Phys. Rev. B **14**, 4946 (1976).
[8] D. Furman, S. Dattagupta, and R. B. Griffiths, Phys. Rev. B **15**, 441 (1977).
[9] Y. L. Wang and D. Rauchwarger, Phys. Lett. **59A**, 73 (1976).
[10] J. D. Kimel, S. Black, P. Carter, and Y. L. Wang, Phys. Rev. B **35**, 3347 (1987).
[11] R. B. Griffiths, Physica **33**, 690 (1967).
[12] F. Y. Wu, Chin. J. Phys. **16**, 153 (1976).
[13] T. Horiguchi, Phys. Lett. **113A**, 425 (1986).
[14] F. Y. Wu, Phys. Lett. A **116**, 245 (1986).
[15] R. Shankar, Phys. Lett. A **117**, 365 (1986).
[16] X. N. Wu and F. Y. Wu, J. Stat. Phys. **50**, 41 (1988).
[17] F. Y. Wu, X. N. Wu, and H. W. J. Blöte, Phys. Rev. Lett. **62**, 2773 (1989).
[18] X. N. Wu and F. Y. Wu, Phys. Lett. A **144**, 123 (1990).
[19] H. W. J. Blöte and X. N. Wu, J. Phys. A **23**, L627 (1990).
[20] L. H. Gwa, Phys. Rev. Lett. **63**, 1440 (1989).
[21] L. H. Gwa, Phys. Rev. B **41**, 7315 (1990).
[22] L. H. Gwa and F. Y. Wu, J. Phys. A (to be published).
[23] M. N. Barber, in *Phase Transitions and Critical Phenomena,* edited by C. Domb and J. L. Lebowtiz (Academic, New York, 1983), Vol. 8.
[24] V. Privman and M. E. Fisher, Phys. Rev. B **30**, 1766 (1988).
[25] M. E. Fisher, in *Critical Phenomena,* Proceedings of the International School of Physics, "Enrico Fermi," Course 51, edited by M. S. Green (Academic, New York, 1971).
[26] H. W. J. Blöte, F. Y. Wu, and X. N. Wu, Int. J. Mod. Phys. B **4**, 619 (1990).
[27] F. Y. Wu, Rev. Mod. Phys. **54**, 235 (1982).